International Journal of Current Engineering and Technology
E-ISSN 2277 – 4106, P-ISSN 2347 - 5161

Available at http://inpressco.com/category/ijcet

Research Article

A New Multi-Sensor Fusion Strategy for Optimal Spatial Design and Operation of Renewable Energy Grids

Beshoy S. Kest[Å*], Ghada M. Amer[Å], Wael A. Mohamed[Å] and Hassen T. Dorrah[B]

[Å]Electrical Engineering Department, Benha Faculty of Engineering, Benha University, Qalubia, Egypt
[B]Electrical Engineering Department, Faculty of Engineering, Cairo University, Giza, Egypt

Accepted 20 Dec 2014, Available online 25 Dec 2014, **Vol. 4, No.6 (Dec 2014)**

Abstract

This paper provides a new technique of multi-sensor data fusion to achieve an optimal spatial design and power operation of integrated Renewable Energy Grids (REG). This new approach depends on making a sensor data fusion system depending on the spatial concepts for measuring the important climate parameters, which have a great effect on the performance of REG. This methodology has been designed around spatial concept to reach the optimal operation continuously. The spatial concept has a successful relationship with power energy smart grids. Wireless reliable sensors-based network configuration has been developed around the power stations locations to provide online-required operational climate data to supply the algorithm with necessitated measured data. The realistic procedure of the wireless reliable climate sensors networks in terms of the locations, number and types of sensors and the method of dealing with are analyzed. To test the feasibility of sensors data fusion system, a practical case study in Egypt is applied. Moreover, a missing sensor data case is discussed and its results have been included.

Keywords: *Photovoltaic Systems, Sensor Fusion, Smart Grids, Spatial Concept, Wind Farms, Wireless Sensor Networks.*

1. Introduction

Renewable energy is accepted as a key source for the future (Nicola Miles and Kathleen Odell, 2004). This is primarily due to fact that renewable energy resources have some advantages when compared to fossil fuels (Taha Ahmed Tawfik Hussein, 2012). Renewable energy technologies are clean sources of energy that have a much lower environmental impact than conventional energy technologies. While some countries have adequate renewable energy potential, which enable them to make integrated renewable energy grids, which can support their energy demand, it is therefore important to harness that resource in view to find solution to energy shortage and environmental degradation the countries are being faced to (El-Metwally M. , 2005).

To maximize the benefits of integrated renewable energy grids to achieve the maximum power operation, a multi-sensor data fusion system is developed around a spatial design for some important climate parameters. Data fusion is the process of combing information from a number of different spatial sources to provide a robust and complete description of an environment or process of interest. There has been much research on the subject of multi-sensor data fusion in recent years, due to its potential advantages (Jaime Esteban, *et al*, 2005), which can reduce overall uncertainty and thus serve to increase the accuracy with which the features are perceived by the system. Multiple sensors providing redundant information can also serve to increase reliability in the case of sensor error or failure.

Complementary information from multiple sensors allows features in the environment to be perceived that are impossible to perceive using just the information from each individual sensor operating separately (Ren C. Luo, *et al*, 2002). Multi-sensor data fusion tries to replicate the work performed by our brain–it takes information acquired by a number of different sensors and fuses it together, taking advantage of different points of view.

To gather this information, different type wireless sensors networks (WSN) are equipped and generally established in the desired locations, which are needed to know the measurements at. A wireless sensor network of spatially distributed autonomous sensors to monitor physical or environmental conditions, such as temperature, Radiation, Wind velocity, sound, pressure, etc. and to cooperatively pass their data through the network to a main location. The development of wireless sensor networks was motivated by such networks are used in many weather and industrial applications, such as environment parameter monitoring, industrial process control, and machine health monitoring.

The main purpose of this paper is to reach a new technique of multi-sensor data fusion to control on power operation of renewable energy power grids via wireless sensor networks. The main function of (WSN) is to gather climate information in a day such as air temperature T, wind velocity V and solar radiation R.

*Corresponding author: **Beshoy S. Kest**

This paper is organized as follows: Section 2 discusses the theory of multi-sensor data fusion. Section 3 explains the proposed sensor fusion algorithm and its different models. A practical case study in Egypt is applied in section 4. Section 5 shows the realistic expected procedures of the fusion system by using Wireless Sensor Network. Section 6 displays software tools and model inputs. Section 7 discusses the simulation results of the proposed sensor fusion approach. Section 8 discusses the missing sensor data case. Finally, Section 9 presents brief conclusion.

2. Sensor fusion technique

A multi-sensor data fusion system has three main components, Sensors, Sensor data processing, Data fusion. Each component represents an individual stage over all the system. Figure 1, gives a brief depict of a simple multi-sensor data fusion system. The sensors in a multi-sensor data fusion system depend heavily on the application for which the system is built. The number of sensors used is an important factor in the cost equation in terms of time, money and effort and should be limited by the information gained. Identical sensors are used within the multi-sensor system then the data analysis process can be done with minimal effort (Martin E. Liggins, *et al*, 2009). This can enhance the reliability of the results provided by the redundancy of the information. The reliability of the data used within the fusion system will depend on the sensors available and the methodology employed for the fusion of the data. The selection of sensors and its number increases the accuracy of the information transferred.

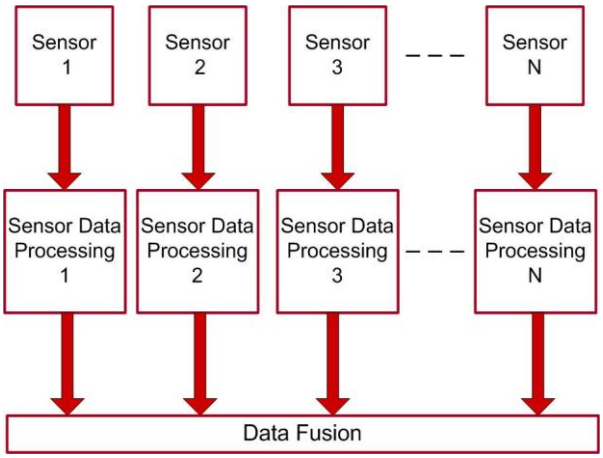

Fig.1 A simple multi-sensor data fusion system

3. Proposed sensor fusion algorithm

The multi-sensor data fusion strategy, which will be used, depends on many parameters in the sensor system. All these parameters are appeared in the algorithm to make a complete data fusion system.

3.1 Algorithm configuration

The system consists of a number of sensor S which are linked together to form three wireless sensors networks such as; temperature sensor network, wind velocity sensor network and solar radiation network in addition, the power stations which need to make a sensor fusion at its location. Figure 2, gives a brief depict of the used multi-sensor data fusion algorithm. The multi-sensor fusion proposed algorithm relies on many factors; both the formula and the relationship between the measured amount type by sensor and the maximum power of power station, the distance L, between a sensor location, the power station location, and the accuracy of the used sensors.

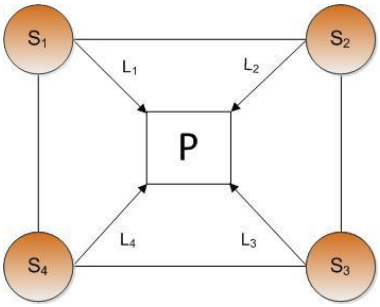

Fig.2 The used multi-sensor data fusion algorithm

Where S_j represents the sensor number and P is a location of power station.

At the location of power station P, the data fusion formula is shown in equation (1).

$$P = \frac{\frac{S_1}{L_1} + \frac{S_2}{L_2} + \frac{S_3}{L_3} + \frac{S_4}{L_4}}{\frac{1}{L_1} + \frac{1}{L_2} + \frac{1}{L_3} + \frac{1}{L_4}} \quad (1)$$

In a general case, the equation (1) may be generalized and modified to comprehend n numbers of sensors as the following in equation (2).

$$P = \frac{\frac{S_1}{L_1} + \frac{S_2}{L_2} + \frac{S_3}{L_3} + \frac{S_4}{L_4} + \ldots + \frac{S_n}{L_n}}{\frac{1}{L_1} + \frac{1}{L_2} + \frac{1}{L_3} + \frac{1}{L_4} + \ldots + \frac{1}{L_n}} \quad (2)$$

In case there are corrupted or faulty data coming from any sensor, a new parameter will be added in the equation to avoid this fault or the corrupted data, modify the response and improve the behavior and result of the system. Alpha α is a new parameter, positive value, will be add as an exponent of distances. The equation (2) will be modified to become (3).

$$P = \frac{\frac{S_1}{L_1^{\alpha 1}} + \frac{S_2}{L_2^{\alpha 2}} + \frac{S_3}{L_3^{\alpha 3}} + \frac{S_4}{L_4^{\alpha 4}} + \ldots + \frac{S_n}{L_n^{\alpha n}}}{\frac{1}{L_1^{\alpha 1}} + \frac{1}{L_2^{\alpha 2}} + \frac{1}{L_3^{\alpha 3}} + \frac{1}{L_4^{\alpha 4}} + \ldots + \frac{1}{L_n^{\alpha n}}} \quad (3)$$

where α is an exponent of distance.

To explain the fusion algorithm extensively, a larger multi-sensor data fusion system is considered. This example contains five sensors and three power stations.

In Figure 3, there are many power stations; each power station is presented by an equation. Therefore, the number of equations equals the number locations of power stations.

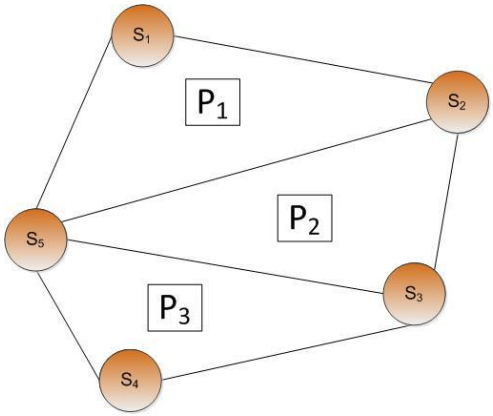

Fig. 3 A larger multi-sensor data fusion system

• Location Power Station P_1:
The data fusion algorithm formula at the location of power station P_1 is demonstrated in equation (4). Figure 4, shows the distances between power station P_1 and all sensors.

$$P_1 = \frac{\frac{S_1}{L_{11}{}^{\alpha 1}} + \frac{S_2}{L_{12}{}^{\alpha 2}} + \frac{S_3}{L_{13}{}^{\alpha 3}} + \frac{S_4}{L_{14}{}^{\alpha 4}} + \frac{S_5}{L_{15}{}^{\alpha 5}}}{\frac{1}{L_{11}{}^{\alpha 1}} + \frac{1}{L_{12}{}^{\alpha 2}} + \frac{1}{L_{13}{}^{\alpha 3}} + \frac{1}{L_{14}{}^{\alpha 4}} + \frac{1}{L_{15}{}^{\alpha 5}}} \quad (4)$$

where L_{ij} is the distance between P_i and S_j.

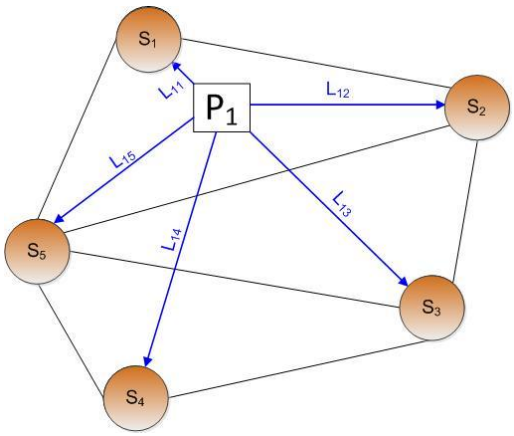

Fig. 4 The distances between location of P_1 and all sensors

• Location Power Station P_2:
The data fusion algorithm formula at the location of power station P_2 is demonstrated in equation (5). Figure 5, shows the distances between power station P_2 and all sensors.

$$P_2 = \frac{\frac{S_1}{L_{21}{}^{\alpha 1}} + \frac{S_2}{L_{22}{}^{\alpha 2}} + \frac{S_3}{L_{23}{}^{\alpha 3}} + \frac{S_4}{L_{24}{}^{\alpha 4}} + \frac{S_5}{L_{25}{}^{\alpha 5}}}{\frac{1}{L_{21}{}^{\alpha 1}} + \frac{1}{L_{22}{}^{\alpha 2}} + \frac{1}{L_{23}{}^{\alpha 3}} + \frac{1}{L_{24}{}^{\alpha 4}} + \frac{1}{L_{25}{}^{\alpha 5}}} \quad (5)$$

• Location Power Station P_3:
The data fusion algorithm formula at the location of power station P_3 is demonstrated in equation (6). Figure 6, shows the distances between power station P_3 and all sensors.

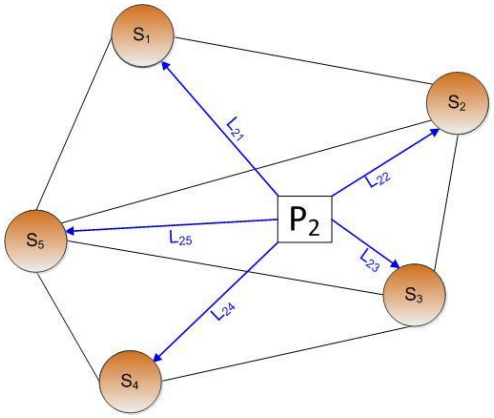

Fig. 5 The distances between location of P_2 and all sensors

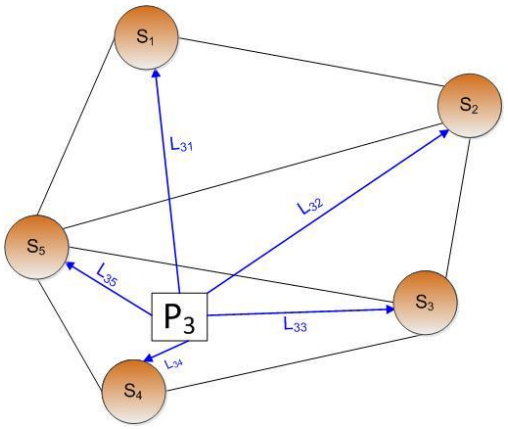

Fig. 6 The distances between location of P_3 and all sensors

$$P_3 = \frac{\frac{S_1}{L_{31}{}^{\alpha 1}} + \frac{S_2}{L_{32}{}^{\alpha 2}} + \frac{S_3}{L_{33}{}^{\alpha 3}} + \frac{S_4}{L_{34}{}^{\alpha 4}} + \frac{S_5}{L_{35}{}^{\alpha 5}}}{\frac{1}{L_{31}{}^{\alpha 1}} + \frac{1}{L_{32}{}^{\alpha 2}} + \frac{1}{L_{33}{}^{\alpha 3}} + \frac{1}{L_{34}{}^{\alpha 4}} + \frac{1}{L_{35}{}^{\alpha 5}}} \quad (6)$$

It is possible to write the equations (4) to (6) together in a matrix form to express the conclusion of the system as in equation (7), where, the L.H.S is a vector of P, which is m x 1, and the R.H.S is consisted of a matrix m x n and a vector of sensor n x 1.

$$\begin{bmatrix} P_1 \\ P_2 \\ P_3 \end{bmatrix} = \begin{bmatrix} \frac{1}{L_{11}{}^{\alpha 1}} & \frac{1}{L_{12}{}^{\alpha 2}} & \frac{1}{L_{13}{}^{\alpha 3}} & \frac{1}{L_{14}{}^{\alpha 4}} & \frac{1}{L_{15}{}^{\alpha 5}} \\ \hline Y_1 & Y_1 & Y_1 & Y_1 & Y_1 \\ \frac{1}{L_{21}{}^{\alpha 1}} & \frac{1}{L_{22}{}^{\alpha 2}} & \frac{1}{L_{23}{}^{\alpha 3}} & \frac{1}{L_{24}{}^{\alpha 4}} & \frac{1}{L_{25}{}^{\alpha 5}} \\ \hline Y_2 & Y_2 & Y_2 & Y_2 & Y_2 \\ \frac{1}{L_{31}{}^{\alpha 1}} & \frac{1}{L_{32}{}^{\alpha 2}} & \frac{1}{L_{33}{}^{\alpha 3}} & \frac{1}{L_{34}{}^{\alpha 4}} & \frac{1}{L_{35}{}^{\alpha 5}} \\ \hline Y_3 & Y_3 & Y_3 & Y_3 & Y_3 \end{bmatrix} \begin{bmatrix} S_1 \\ S_2 \\ S_3 \\ S_4 \\ S_5 \end{bmatrix} \quad (7)$$

where Y_1 is the denominator of the equation (4), as in equation (8).

$$Y_1 = \frac{1}{L_{11}{}^{\alpha 1}} + \frac{1}{L_{12}{}^{\alpha 2}} + \frac{1}{L_{13}{}^{\alpha 3}} + \frac{1}{L_{14}{}^{\alpha 4}} + \frac{1}{L_{15}{}^{\alpha 5}} \quad (8)$$

Similarly, the denominator of the equation (5) is Y_2 and the denominator of the equation (6) is Y_3.

The matrix, in equation (7), can be generalized and modified to include number n sensors and number m Power stations, as following in equation (9).

$$\begin{bmatrix} P_1 \\ P_2 \\ P_3 \\ \vdots \\ P_m \end{bmatrix} = \begin{bmatrix} \frac{1}{L_{11}{}^{\alpha 1}} & \frac{1}{L_{12}{}^{\alpha 2}} & \frac{1}{L_{13}{}^{\alpha 3}} & \frac{1}{L_{14}{}^{\alpha 4}} & \frac{1}{L_{15}{}^{\alpha 5}} & \cdots & \frac{1}{L_{1n}{}^{\alpha n}} \\ \hline Y_1 & Y_1 & Y_1 & Y_1 & Y_1 & & Y_1 \\ \frac{1}{L_{21}{}^{\alpha 1}} & \frac{1}{L_{22}{}^{\alpha 2}} & \frac{1}{L_{23}{}^{\alpha 3}} & \frac{1}{L_{24}{}^{\alpha 4}} & \frac{1}{L_{25}{}^{\alpha 5}} & \cdots & \frac{1}{L_{2n}{}^{\alpha n}} \\ \hline Y_2 & Y_2 & Y_2 & Y_2 & Y_2 & & Y_2 \\ \frac{1}{L_{31}{}^{\alpha 1}} & \frac{1}{L_{32}{}^{\alpha 2}} & \frac{1}{L_{33}{}^{\alpha 3}} & \frac{1}{L_{34}{}^{\alpha 4}} & \frac{1}{L_{35}{}^{\alpha 5}} & \cdots & \frac{1}{L_{3n}{}^{\alpha n}} \\ \hline Y_3 & Y_3 & Y_3 & Y_3 & Y_3 & & Y_3 \\ \vdots & \vdots & \vdots & \vdots & \vdots & \ddots & \vdots \\ \frac{1}{L_{m1}{}^{\alpha 1}} & \frac{1}{L_{m2}{}^{\alpha 2}} & \frac{1}{L_{m3}{}^{\alpha 3}} & \frac{1}{L_{m4}{}^{\alpha 4}} & \frac{1}{L_{m5}{}^{\alpha 5}} & \cdots & \frac{1}{L_{2n}{}^{\alpha n}} \\ \hline Y_m & Y_m & Y_m & Y_m & Y_m & & Y_m \end{bmatrix} \begin{bmatrix} S_1 \\ S_2 \\ S_3 \\ S_4 \\ S_5 \\ \vdots \\ S_n \end{bmatrix} \quad (9)$$

where Y_1 is, as equation (10).

$$Y_1 = \frac{1}{L_{11}{}^{\alpha 1}} + \frac{1}{L_{12}{}^{\alpha 2}} + \frac{1}{L_{13}{}^{\alpha 3}} + \frac{1}{L_{14}{}^{\alpha 4}} + \frac{1}{L_{15}{}^{\alpha 5}} + \cdots + \frac{1}{L_{1n}{}^{\alpha n}} \quad (10)$$

Similarly, the denominators Y_2 and Y_3.

3.2 Algorithm development

To make a comprehensive expression of the data fusion proposed algorithm, the weight expression is utilized, where the distance between any sensor and any power station can be considered as a weight of the sensor as in equation (11). This weight w and W explains how the data of the sensor effect on the location of power station.

$$\begin{bmatrix} P_1 \\ P_2 \\ P_3 \\ \vdots \\ P_m \end{bmatrix} = \begin{bmatrix} \frac{w_{11}}{W_1} & \frac{w_{12}}{W_1} & \frac{w_{13}}{W_1} & \frac{w_{14}}{W_1} & \frac{w_{15}}{W_1} & \cdots & \frac{w_{1n}}{W_1} \\ \frac{w_{21}}{W_2} & \frac{w_{22}}{W_2} & \frac{w_{23}}{W_2} & \frac{w_{24}}{W_2} & \frac{w_{25}}{W_2} & \cdots & \frac{w_{2n}}{W_2} \\ \frac{w_{31}}{W_3} & \frac{w_{32}}{W_3} & \frac{w_{33}}{W_3} & \frac{w_{34}}{W_3} & \frac{w_{35}}{W_3} & \cdots & \frac{w_{3n}}{W_3} \\ \vdots & \vdots & \vdots & \vdots & \vdots & \ddots & \vdots \\ \frac{w_{m1}}{W_m} & \frac{w_{m2}}{W_m} & \frac{w_{m3}}{W_m} & \frac{w_{m4}}{W_m} & \frac{w_{m5}}{W_m} & \cdots & \frac{w_{mn}}{W_m} \end{bmatrix} \begin{bmatrix} S_1 \\ S_2 \\ S_3 \\ S_4 \\ S_5 \\ \vdots \\ S_n \end{bmatrix} \quad (11)$$

Where $w_{ij} = \frac{1}{L_{ij}{}^{\alpha j}}$ is the weight between P_i and S_j.

The denominator W_1 is expressed as in equation (12).

$$W_1 = w_{11} + w_{12} + w_{13} + w_{14} + w_{15} + \cdots + w_{1n} \quad (12)$$

Similarly, the denominators W_2 and W_3.

4. Case study

To check the credibility of the suggested technique, it should be checked on a practical case study. Actually, there is not found a good case study except that is existed in Egypt. With the expected depletion of natural gas reserves within the next 57 years, Egypt is an investor's dream when it comes to sustainable energy resources. Egypt possesses an abundance of land, sunny weather and high wind speed, making it a prime resource for two renewable energy sources: wind, solar (GAFI, 2013).

4.1 Case study description

The geographical environment of Egypt generally, on the Red Sea Beach specifically enables it to be one of the best places to invest in Renewable Energy Power Grids. Indeed, Egypt has many Renewable Energy Grids long as the Red Sea Beach from the Suez Governorate in North until Safaga City in South.

On the Red Sea beach, there are many Renewable Power Stations such as;

- Zaafarana Wind Power Station 545 MW P_1.

The largest wind farm on the African continent, it has been being operating since 2001. It is located 120 km south of Suez on the Red Sea, the park currently boasts a capacity of 80 MW and is delivering total output of 545 MW as of 2011.

- Hurghada Solar Power Station 10.5 MW P_2.
- Hurghada Wind Power Station 5 MW P_3.(NREA, 2013)

Hurghada wind farm includes wind turbines with different technologies; manufacturing. Wind turbines have single, double and triple blades. The percentage of local manufacturing in this plant reached about 40% (blades, towers, mechanical and electrical works), saving about 1.5 thousand tons of oil equivalents, and reducing the emission of about 4000 tons of carbon dioxide.

- Suez Gulf Wind Power Station 200 MW P_4.

All these renewable power station are overlooking on Red Sea beach. These Renewable Power Stations will be considered as the power stations P_i in the multi sensor data fusion's algorithm.

It is worth mentioning that Temperature sensors, Wind velocity sensors and Radiation sensors are selected because of the relationship between the measured parameter of each sensor and the maximum power that can be obtained from the renewable power stations whether solar power station or wind power station. It is needed to build three sensor networks as temperature sensor network, wind velocity sensor network, and radiation sensor network around these power stations to feed the information from the sensors to Multi Sensor Data Fusion's algorithm. The sensors of these networks are distributed in six locations as in Table 1 and Figure 7.

Table 1 The distribution of the sensors in six places

Locations	A	B	C	D	E	F
Temperature Sensor T	✓	✓	✓	✓	✓	✓
Wind velocity Sensor V	✓	--	✓	✓	✓	✓
Radiation Sensor R	✓	--	✓	✓	✓	--

(A. Suez, B. Ain El Sokhna, C. Zaafarna, D. Ras Gahrib, E. Hurghada and F. Safaga)

The majority of locations contain the three types of sensors such as; locations A, C, D and E. Only, one location contains a two type of sensors as location F and location B contains only one sensor.

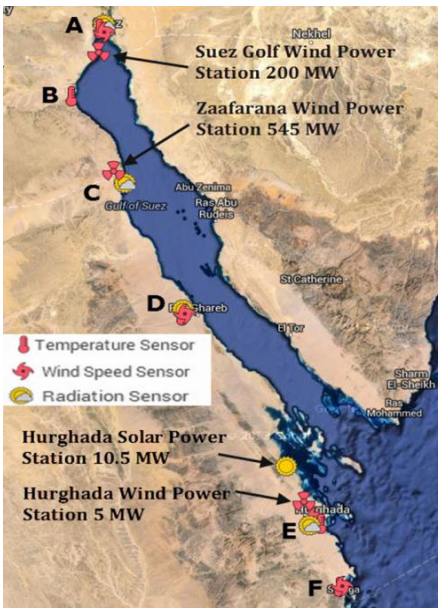

Fig. 7 Locations of renewable energy power stations overlooking on the red sea and sensors networks

4.2 Case study models

According to the algorithm and the different types of sensors that are used, every sensor has a unique model. Therefore, the three mathematical different models related to three different sensors types are adapted for a case study.

Temperature sensors network model, wind velocity sensors network model and radiation sensors network model in terms of the weight are reached after substitution in equations (11) by number of power station m and the number of sensors n in each network, as in equation (13) to (15).

1. Temperature Sensors Network T:

$$\begin{bmatrix} T_{P1} \\ T_{P2} \\ T_{P3} \\ T_{P4} \end{bmatrix} = \begin{bmatrix} \frac{w_{11}}{W_1} & \frac{w_{12}}{W_1} & \frac{w_{13}}{W_1} & \frac{w_{14}}{W_1} & \frac{w_{15}}{W_1} & \frac{w_{16}}{W_1} \\ \frac{w_{21}}{W_2} & \frac{w_{22}}{W_2} & \frac{w_{23}}{W_2} & \frac{w_{24}}{W_2} & \frac{w_{25}}{W_2} & \frac{w_{26}}{W_2} \\ \frac{w_{31}}{W_3} & \frac{w_{32}}{W_3} & \frac{w_{33}}{W_3} & \frac{w_{34}}{W_3} & \frac{w_{35}}{W_3} & \frac{w_{36}}{W_3} \\ \frac{w_{41}}{W_4} & \frac{w_{42}}{W_4} & \frac{w_{43}}{W_4} & \frac{w_{44}}{W_4} & \frac{w_{45}}{W_4} & \frac{w_{46}}{W_4} \end{bmatrix} \begin{bmatrix} S_{T1} \\ S_{T2} \\ S_{T3} \\ S_{T4} \\ S_{T5} \\ S_{T6} \end{bmatrix} \quad (13)$$

2. Wind Velocity Sensors Network V:

$$\begin{bmatrix} V_{P1} \\ V_{P2} \\ V_{P3} \\ V_{P4} \end{bmatrix} = \begin{bmatrix} \frac{w_{11}}{W_1} & \frac{w_{12}}{W_1} & \frac{w_{13}}{W_1} & \frac{w_{14}}{W_1} & \frac{w_{15}}{W_1} \\ \frac{w_{21}}{W_2} & \frac{w_{22}}{W_2} & \frac{w_{23}}{W_2} & \frac{w_{24}}{W_2} & \frac{w_{25}}{W_2} \\ \frac{w_{31}}{W_3} & \frac{w_{32}}{W_3} & \frac{w_{33}}{W_3} & \frac{w_{34}}{W_3} & \frac{w_{35}}{W_3} \\ \frac{w_{41}}{W_4} & \frac{w_{42}}{W_4} & \frac{w_{43}}{W_4} & \frac{w_{44}}{W_4} & \frac{w_{45}}{W_4} \end{bmatrix} \begin{bmatrix} S_{V1} \\ S_{V2} \\ S_{V3} \\ S_{V4} \\ S_{V5} \end{bmatrix} \quad (14)$$

3. Radiation Sensors Network R:

$$\begin{bmatrix} R_{P1} \\ R_{P2} \\ R_{P3} \\ R_{P4} \end{bmatrix} = \begin{bmatrix} \frac{w_{11}}{W_1} & \frac{w_{12}}{W_1} & \frac{w_{13}}{W_1} & \frac{w_{14}}{W_1} \\ \frac{w_{21}}{W_2} & \frac{w_{22}}{W_2} & \frac{w_{23}}{W_2} & \frac{w_{24}}{W_2} \\ \frac{w_{31}}{W_3} & \frac{w_{32}}{W_3} & \frac{w_{33}}{W_3} & \frac{w_{34}}{W_3} \\ \frac{w_{41}}{W_4} & \frac{w_{42}}{W_4} & \frac{w_{43}}{W_4} & \frac{w_{44}}{W_4} \end{bmatrix} \begin{bmatrix} S_{R1} \\ S_{R2} \\ S_{R3} \\ S_{R4} \end{bmatrix} \quad (15)$$

5. Realistic procedure of the system

Wireless Sensor Networks are emerging as a suitable new tool for a spectrum of new applications in recent years (Chiara Buratti, *et al*, 2009). They are easily deployable at a large scale, low power, inexpensive and self-organizing. These unique characteristics make them advantageous over traditional networks.

Sensor networks applications were originally motivated by military applications such as target detection, surveillance of enemy activities in a battlefield environment and counterterrorism; however, their many advantages over traditional networks resulted in the development of many other potential applications such as; environment and habitat monitoring, health applications, home automation, traffic control and power smart grid as in Figure 8.

The WSN is built of nodes – from a few to several hundreds or even thousands, where each node is connected to one (or sometimes several) sensors. A sensor node should sense, process and communicate the data to wherever it is used with minimum resource consumption. Each such sensor network node has typically several parts: a radio transceiver with an internal antenna or connection to an external antenna, a microcontroller an electronic circuit for interfacing with the sensors. Moreover, integration to a GSM (Global System for Mobile communications)/GPRS (General Packet Radio Service) module to enable communication using the mobile telephone network (D. Gascon, 2010) and an energy source, usually a battery or an embedded form of energy harvesting.

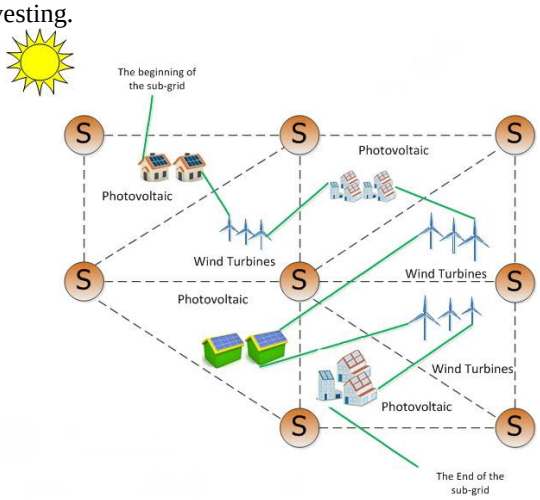

Fig. 8 Power smart grid by using wireless sensors networks

A sensor node should sense, process and communicate the data to wherever it is used with minimum resource consumption (Salem Hadim and Nader Mohamed, 2006). There must be new programming paradigms and new operating systems that glue everything together in an efficient manner, supporting concurrency-intensive operations and insuring robustness and modularity.

A friendly user-programming interface that executes applications and marshals the high-level constructs of the programming language to the low level constructs understandable to the operating system should be provided. The middleware is a suitable tool for this. It should be an unifying layer, integrating the very different components a smart grid is equipped with into one homogeneous-looking layer (José-Fernán Martínez, *et al*, 2013).

It is worth mentioning that the suitable way of implement these different sensors network is by using wireless sensor networks. However, the important issue is how to select the suitable middleware which offering abilities and handle the challenges of (WSN). Indeed the need for a middleware layer that fully meets the design and implementation of different challenges of sensor network technologies is a novel approach to resolve many of the open issues and drastically enhance the development of applications on such networks. (D. Estrin, *et al*, 1999)

The design and development of a successful middleware layer for WSN is not trivial. It needs to deal with many challenges dictated by WSN characteristics on one hand and the applications on the other hand. (J. Heideman, *et al*, 2001)

a) Hardware resources.
b) Scalability and network topology.
c) Heterogeneity.
d) Network organization.
e) Real-world Integration.
f) Application knowledge.

Some design principles and research projects of Middleware for Sensor Networks have already been proposed. All these different approaches of middleware are presented in details and evaluated to explore the pros and cons in (P. Levis and D. Culler, 2002), (R. Barr, *et al*,2002), (W.B. Heinzelman, *et al*, 2004), (Yong Yao, 2006), (X. Yu, *et al*, 2003).

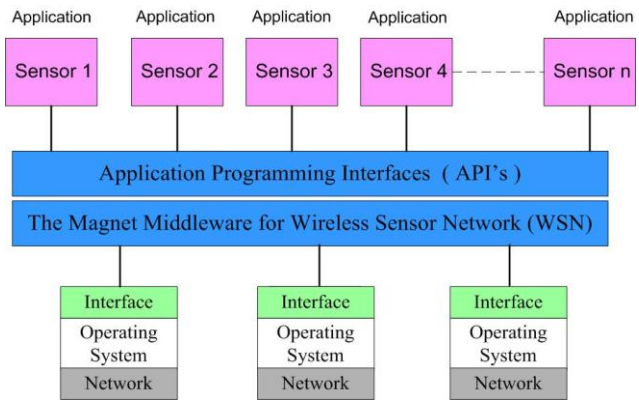

Fig. 9 The magnet middleware architecture for sensors in wireless sensors networks (WSN)

A state of the art comparison and classification by concentrating on similarities and differences between the approaches are provided. Middleware approaches for WSN are mainly classified into three categories: virtual machine, database based and application driven.

Further, it is worth mentioning that the Mate and Magnet middleware are suitable to work in the used Wireless Sensor Network in this power grid system. However, Mate is suitable for a sleepy application because its consuming high power, for complex applications, it is wasteful because of the interpretation overhead. Thus, the Magnet middleware is preferable for the meteorological stations Wireless Sensor Networks as shown in Figure 9, because it is not need to high power, but it uses java virtual machine that introduces an overhead in its instructions.

6. Software tools and model inputs

The three models of multi sensor fusion technique was designed for Temperature sensors network, wind velocity sensors Network and radiation sensors network by using MatLab/Simulink toolbox, which is an interactive tool for modeling, simulating and analyzing dynamic systems (Steven T. Karris, 2006). Simulink provides a complete set of modeling tools that can be used to quickly develop detailed block diagrams of the systems. It integrates seamlessly with MATLAB or any simulation software package, providing the user with immediate access to an extensive range of analysis. Simulink enables the building of graphical block diagrams, simulate dynamic systems, evaluate system performance and refine the designs. The model inputs include parameters supplied by the user such as the distances between the sensor locations and power stations, the simulation time, value of Alfa α and measured data of all sensors at different locations in a certain day, which is used to recognize the required estimated reading.

7. Simulation Result

7.1 Temperature Sensor Network

Figure 10, shows the measured reading of all temperature sensors S_{T1}, S_{T2}, S_{T3}, S_{T4}, S_{T5} and S_{T6}. These measured readings of all sensors are taken over 24 hours in a day.

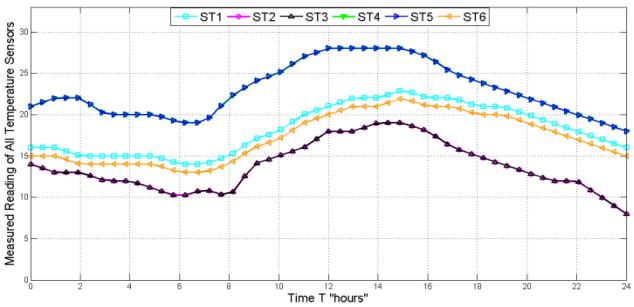

Fig. 10 The measured readings of all temperature sensors S_{T1}, S_{T2}, S_{T3}, S_{T4}, S_{T5} and S_{T6}

In a deep view to Figure 10, it is noted the measured data that are sent from the temperature sensors network are not

equal the number of temperature sensors because sensors S_{T2} and S_{T3} have the same measured reading data. They appear as one black line. Moreover, sensors S_{T4} and S_{T5} have the same measured reading data. They also appear as one blue line.

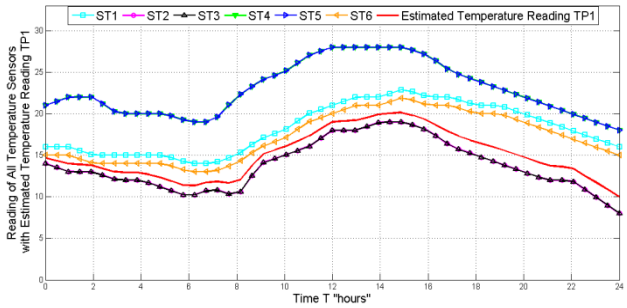

(a) Estimated temperature reading at location of station P_1

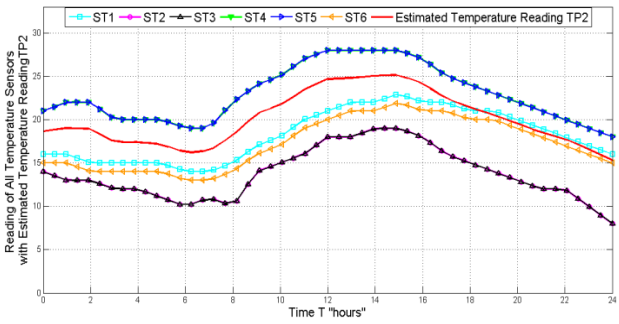

(b) Estimated temperature reading at location of station P_2

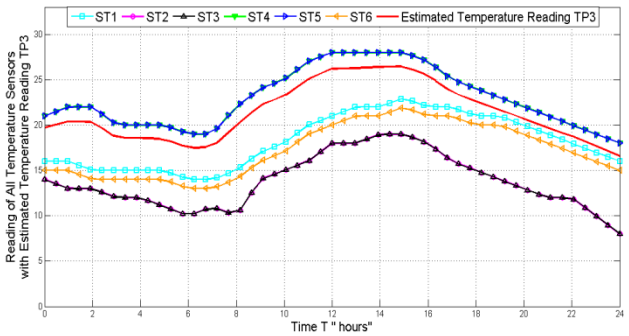

(c) Estimated temperature reading at location of station P_3

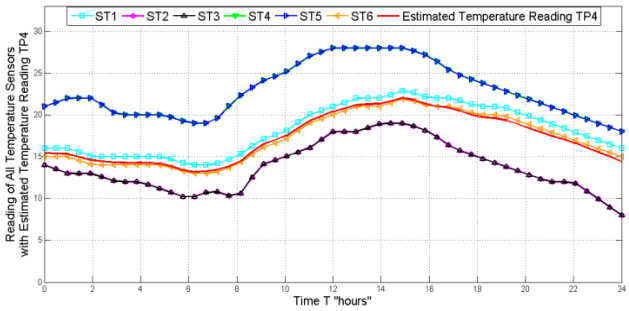

(d) Estimated temperature reading at location of station P_4

Fig. 11 The estimated temperature reading results at the locations at all power stations with measured readings of all temperature sensors

Figure 11, demonstrates the estimated temperature reading results at the locations of all power stations with measured readings of all temperature sensors. These results of the temperature sensors network are produced after making the simulation of its designed model that is in equation (13) and inserting the required distance, measured data of all sensors at different locations and considering the value of Alfa α equals unity.

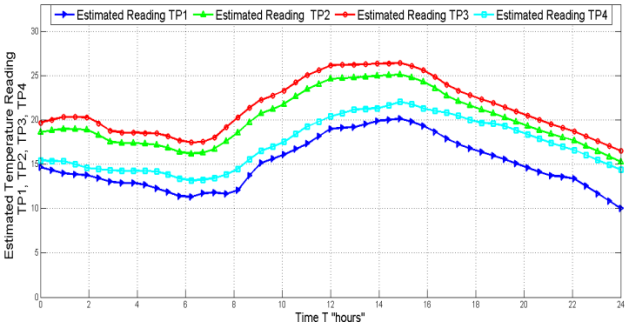

Fig. 12 Estimated temperature reading results at the locations of all power stations P_1, P_2, P_3 and P_4

Figure 12, present the estimated temperature reading results at the locations of all power stations P_1, P_2, P_3 and P_4. It is obvious that power station P_3 Hurghada Wind Power Station and power station P_2 Hurghada Solar Power Station have high estimated reading, which means that these power stations can supply loads more than other power stations.

On the other hand, power station P_4 Suez Gulf Wind Power Station and power station P_1 Zaafarana Wind Power Station come after P_2 respectively, in the value of estimated temperature reading, which means that they can supply less loads than other power stations.

7.2 Wind Velocity Sensors Network

Figure 13, shows the measured reading of all wind velocity sensors S_{V1}, S_{V2}, S_{V3}, S_{V4} and S_{V5}. These measured readings of all sensors are taken over 24 hours in the same day of the temperature sensors readings.

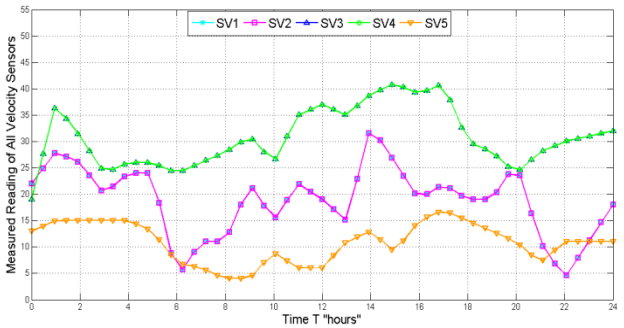

Fig. 13 The measured readings of all wind velocity sensors S_{V1}, S_{V2}, S_{V3}, S_{V4} and S_{V5}

In a comprehensive view to Figure 13, it is remarkable that the measured data that are sent from the wind velocity sensors network are not equal the number of wind velocity sensors, because S_{V1} and S_{V2} have the same data. They appear as one magenta line. Moreover, S_{V3} and S_{V4} have the same data. They also appear as one green line.

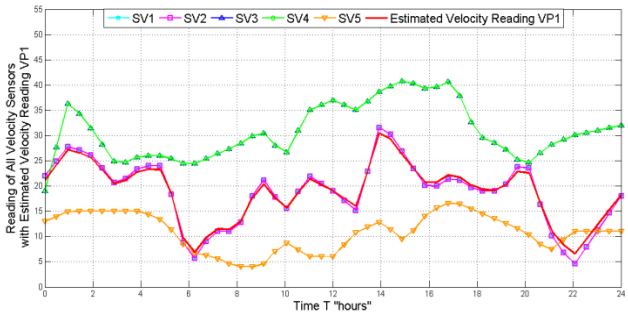

(a) Estimated velocity reading at location of station P_1

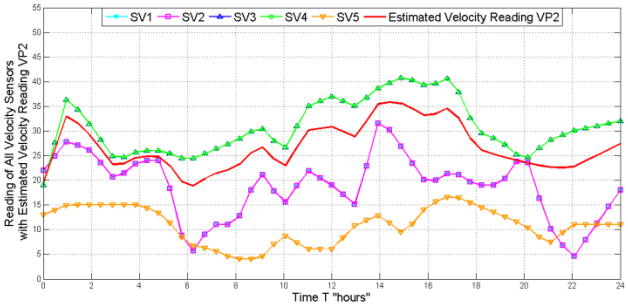

(b) Estimated velocity reading at location of station P_2

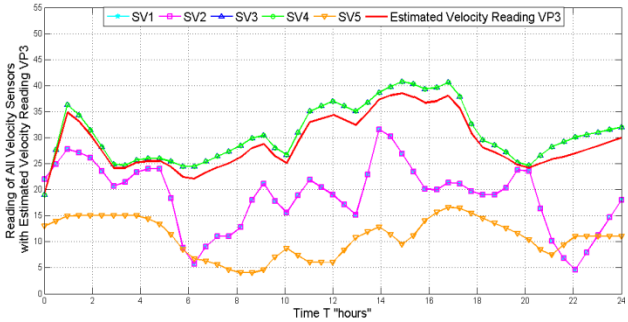

(c) Estimated velocity reading at location of station P_3

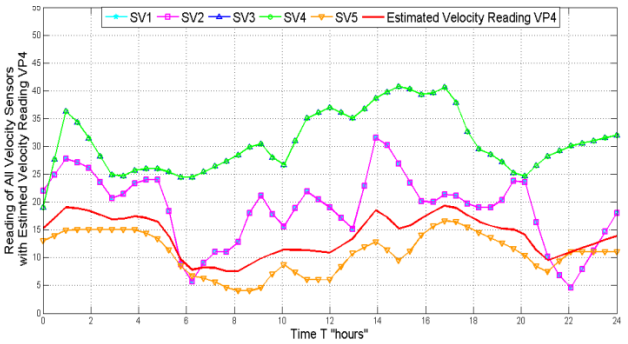

(d) Estimated velocity reading at location of station P_4

Fig. 14 The estimated velocity reading results at the locations of all power stations with measured readings of all wind velocity sensors

Figure 14, elaborates the estimated velocity reading results at the locations of all power stations with measured readings of all wind velocity sensors. These results of wind velocity sensors network are produced under the same conditions of the temperature sensors network however, by using the wind velocity sensor network model that is in equation (14).

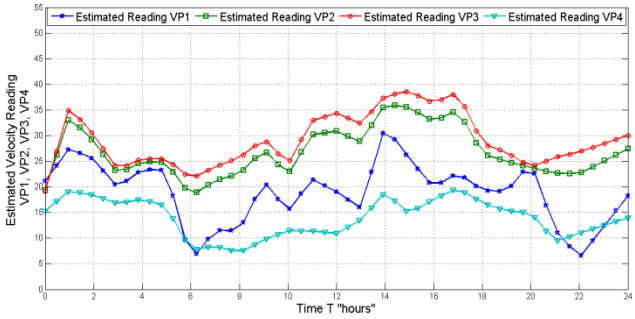

Fig. 15 Estimated velocity reading results at the locations of all power stations P_1, P_2, P_3 and P_4

Figure 15, presents the estimated reading results at the locations of all power stations P_1, P_2, P_3 and P_4. It is easy to conclude that power station P_3 Hurghada Wind Power Station and power station P_2 Hurghada Solar Power Station have high estimated reading with some fluctuation around a day, which means, these power stations can supply loads more than other stations with some fluctuations.

On the other hand, power station P_1 Zaafarana Wind Power Station and power station P_4 Suez Gulf Wind Power Station come after P_2, respectively, in the value of estimated reading, which means that they can supply less loads. However, P_1 down more than P_4 in some Period such as; at 06:00 and from 21:00 to 23:00.

7.3 Radiation Sensors Network

Figure 16, shows the measured reading of all radiation sensors S_{R1}, S_{R2}, S_{R3} and S_{R4}. These measured readings of all sensors are taken over 24 hours in the same day of the temperature sensors readings and wind velocity sensors readings.

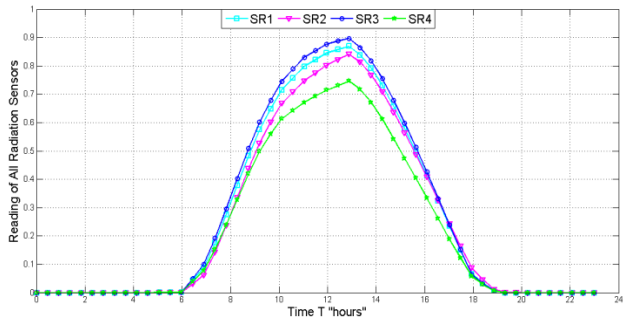

Fig. 16 The measured readings of all radiation sensors S_{R1}, S_{R2}, S_{R3} and S_{R4}

In a concentrated view to Figure16, It indicates the measured data that are sent from the radiation sensors network that are distributed around power stations grids where each curve expresses the data of only one sensor.

Figure 17, displays the estimated radiation reading results at locations of all power stations with measured readings of all radiation sensors. These results of radiation sensors network are produced under the same conditions of the temperature sensor network and wind sensors network however, by using the radiation sensor network model that is in equation (15).

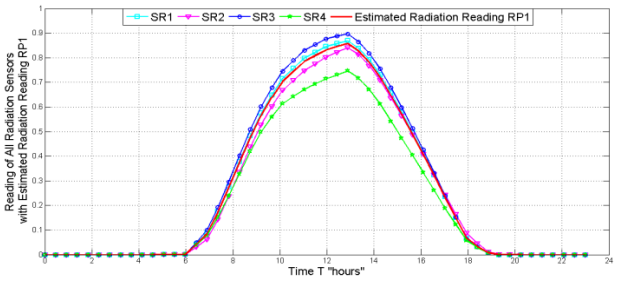

(a) Estimated radiation reading at power station P_1

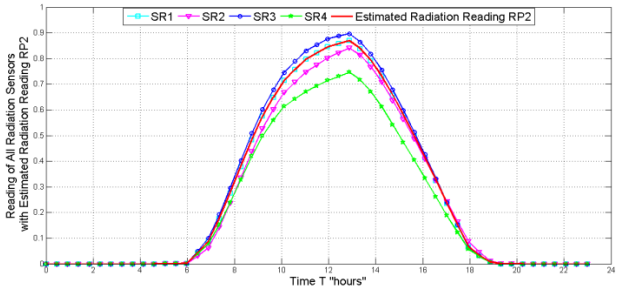

(b) Estimated radiation reading at power station P_2

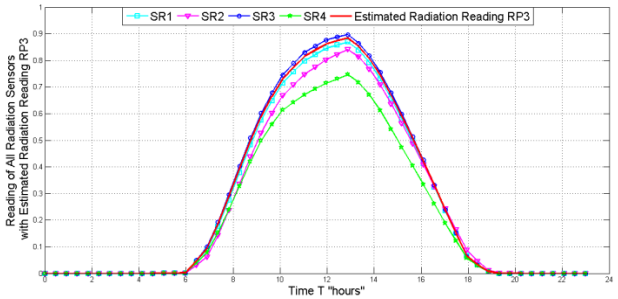

(c) Estimated radiation reading at power station P_3

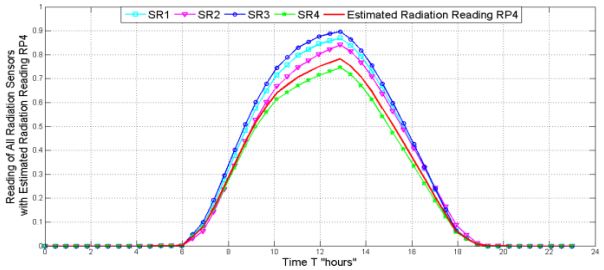

(d) Estimated radiation reading at power station P_4

Fig. 17 The estimated radiation reading results at the locations of all power stations with measured readings of all radiation sensors

Figure 18, illustrates the estimated radiation reading results at the locations of power stations P_1, P_2, P_3 and P_4. It is possible to deduce that power station P_3 Hurghada Wind Power Station has the highest reading between other Power Stations, which indicates that this power station can supply the majority of loads. Power station P_2 Hurghada Solar Power Station and power station P_1 Zaafarana Wind Power Station have approximately the same reading. Then, power station P_4 Suez Gulf Wind Power Station comes in the lowest reading.

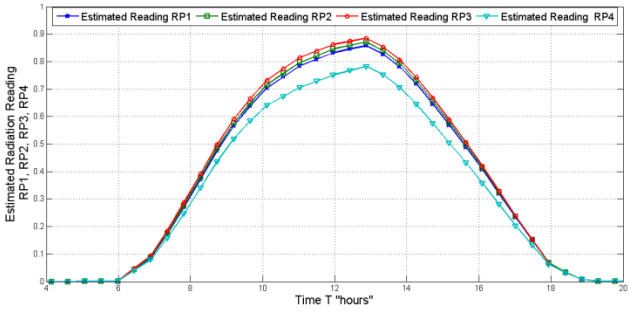

Fig. 18 Estimated radiation reading results at the locations of all power stations P_1, P_2, P_3 and P_4

8. Missing sensor data case

To investigate the system ability, recognize the behavior of the technique and evaluate its reliability at abnormal conditions. A missing sensor data case is considered in each used sensor network, as shown in Figure 19. Accordingly, the data fusion formula at location of power station **P** is as in equation (16). To avoid this defect and to compensate missing data of sensor S_2, the parameter Alfa α does not equal unity as in the normal operation conditions.

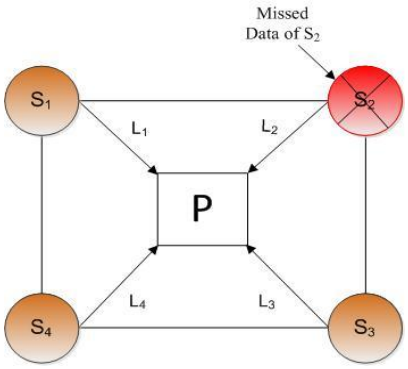

Fig. 19 The fusion system with missed data of sensor S_2

$$P = \frac{\frac{S_1}{L_1^{\alpha 1}} + \frac{S_3}{L_3^{\alpha 3}} + \frac{S_4}{L_4^{\alpha 4}} + \ldots + \frac{S_n}{L_n^{\alpha n}}}{\frac{1}{L_1^{\alpha 1}} + \frac{1}{L_3^{\alpha 3}} + \frac{1}{L_4^{\alpha 4}} + \ldots + \frac{1}{L_n^{\alpha n}}} \quad (16)$$

After making some analyses, It is concluded that the value of α depends on many factors; the used sensor accuracy (i.e. sensor error), the exponent value of the measured parameter of sensor in the P_{max} equation and the coefficient inversely related to correlation factor. Alpha's value is concluded from equation (17).

$$\alpha i = 1 + \varepsilon . r + c \quad (17)$$

Where:

ε is the sensor error; **r** is an exponent of the measured parameter and c is a coefficient inversely related to correlation factor.

In the case study, it is dealing with the three-climate parameters T, R and V due to the relationship between these parameters and the maximum power that can be

obtained from the renewable stations whether solar power station or wind power station, as in equations (18) to (20).

$$P_{\max} = -0.242T + 56.22 \quad (18)$$

$$P_{\max} = 19.147R^2 + 315.27R - 0.79097 \quad (19)$$

$$P_{\max} = 1.3V^3 - 0.44V^2 + 0.15V - 0.00061 \quad (20)$$

In the temperature sensors networks, it is considered that sensors S_2 and S_5 are missed which are nearest sensor and farthest sensor to station P_1, respectively. Similarly, in the wind velocity sensors network, sensors S_1 and S_4 are missed which are nearest sensor and farthest sensor to station P_1, respectively. Similarly, in the Radiation sensors network, sensors S_1 and S_3 are missed which are nearest sensor and farthest sensor to station P_1, respectively. Figures 20, 21 and 22 demonstrate the estimated reading results at the location of power stations P_1 of the temperature, wind velocity and radiation networks, respectively in sensor missed data case.

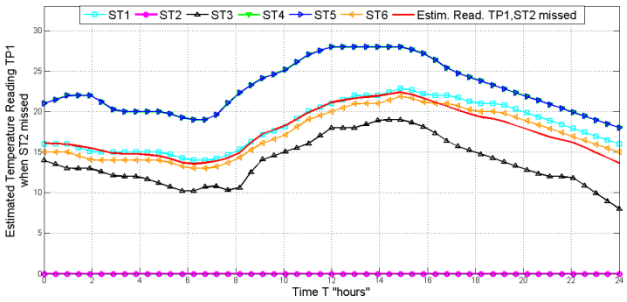

(a) Estimated temperature reading T_{P1}, S_{T2} missed

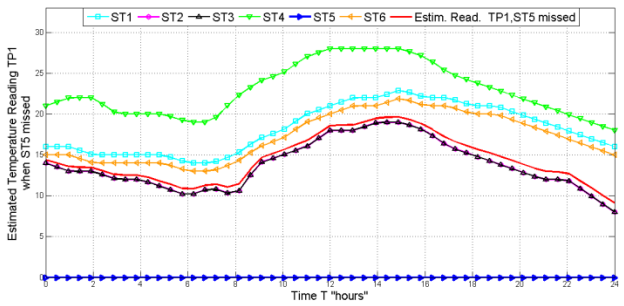

(b) Estimated temperature reading T_{P1}, S_{T5} missed

Fig. 20 Estimated temperature reading results at the location of P_1 of temperature network in sensor missed case

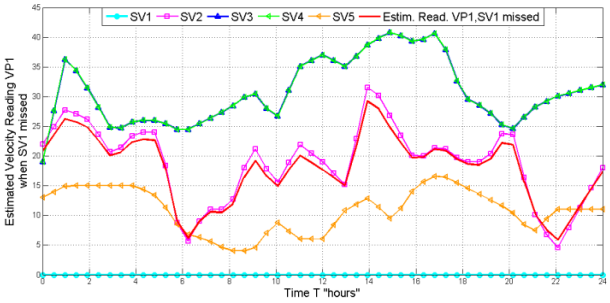

(a) Estimated velocity reading V_{P1}, S_{V1} missed

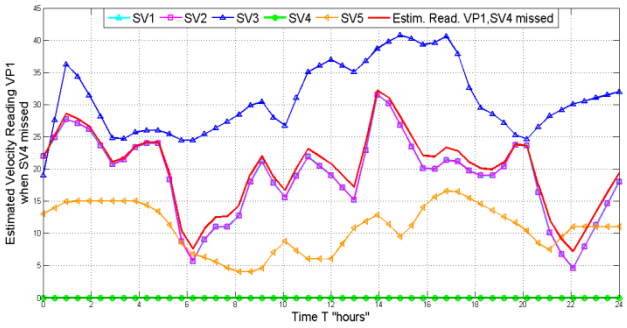

(b) Estimated velocity reading V_{P1}, S_{V4} missed

Fig. 21 Estimated velocity reading results at the location of P_1 of the wind velocity network in sensor missed case.

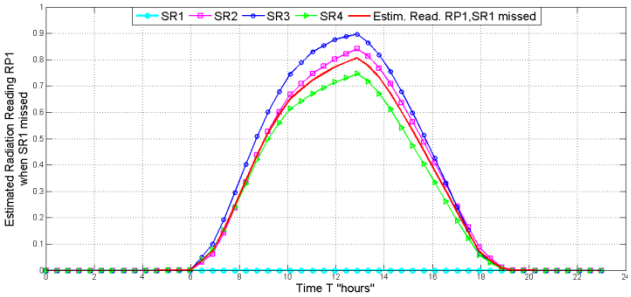

(a) Estimated radiation reading R_{P1}, S_{R1} missed

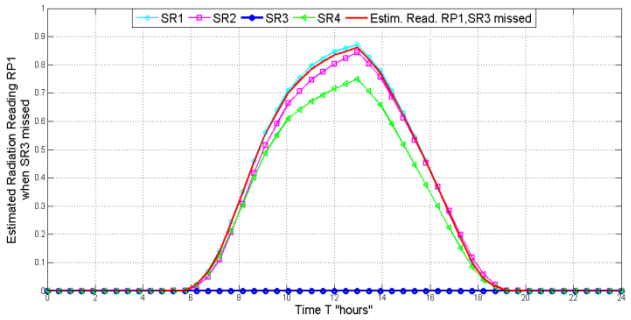

(b) Estimated radiation reading R_{P1}, S_{R3} missed

Fig. 22 Estimated radiation reading results at the location of P_1 of the radiation network in sensor missed case

These results of missing sensor data of all networks are produced after making the simulation of its designed equation that is in equation (16) and inserting the required distance, measured data of all exiting sensors at different locations and considering the value of Alfa α according to equation (17).

In a deducing view to the results in Figures 20, 21 and 22, it is shown that the system tends to follow the next nearest sensor if the nearest one data is missed and follow the nearest sensor in case the farthest one data is missed. Similarly, this behavior occurs for all sensors in between the nearest sensor and the farthest sensor in all different sensors networks.

Conclusion

A model for a new technique of multi-sensor data fusion was proposed in this study. The proposed model can be

used for collecting sufficient data through many different sources depending on and the weighted concept and combined it together, taking into consideration benefits of the spatial concept design, which helps in choosing the power station, which can supply the maximum capacity of loads.

The realistic procedures of the Wireless Sensor Network are discussed and performed to collect the data from the sensors. Selecting the suitable middleware for the Wireless Sensor Network is involved. The model is tested for a case study contains four renewable power stations, which are located at different provinces in Egypt and overlooking on the Red sea beach. It was seen that the simulation results for the model achieved acceptable levels.

A missing sensors data discussion is revealed that the model provides good reliability with a logical behavior of the system. It is expected that this new technique for multi-sensor data fusion will be useful to the engineers of renewable energy related integrated grids.

Acknowledgment

All authors would like to thank Electrical Engineering Department at Benha Faculty of Engineering . In addition, special thanks to Benha University, Qalubia, Egypt. http://www.bu.edu.eg/en/

References

Nicola Miles and Kathleen Odell, (2004), Spatial planning for wind energy: lessons from the Danish case, *Department of Environment, Technology and Social Studies Roskilde Universitets center, Denmark*, pp. 2-9.

Taha Ahmed Tawfik Hussein, (2012), Estimation of hourly global solar radiation in Egypt using mathematical model, *International Journal of Latest Trends in Agriculture & Food Sciences*, Vol. 2, No. 2, pp. 74-82.

El-Metwally M., (2005), Sunshine and global solar radiation estimation at different sites in Egypt, *Journal of Atmospheric and Solar-Terrestrial Physics*, Vol. 67, No. 14, pp.1331–1342.

Jaime Esteban, Andrew Starr, Robert Willetts, Paul Hannah and Peter Bryanston-Cross, (2005), A Review Of Data Fusion Models And Architectures: Towards Engineering Guidelines, *Journal Neural Computing and Applications archive*, Vol. 14, No. 4, pp. 273 – 281.

Ren C. Luo, Chih-Chen Yih, and Kuo Lan Su, (2002), Multisensor Fusion and Integration: Approaches, Applications, and Future Research Directions, *IEEE Sensor Journal*, Vol. 2, No. 2, pp. 107-119.

Martin E. Liggins, David L. Hall and James Llinas, (2009), Handbook of Multisensor Data Fusion Theory and Practice, *Taylor & Francis Group*, pp.1-43.

GAFI (Global Association for Investment) Egyptian Ministry of Investment, Renewable Energy value Report, (2013),www.gafi.gov.eg/content/invsectorsdocs/RenewableEnergyvalue.pdf

NREA (New and Renewable Energy development association), Egyptian Ministry of Electricity, Annual report, (2013), www.nrea.gov.eg/english1.html

Chiara Buratti, Andrea Conti, Davide Dardari and Roberto Verdone, (2009), An Overview on Wireless Sensor Networks Technology and Evolution, *Sensor*, Vol. 9, No. 9, pp. 6869-6896.

D. Gascon, (2010), Long Range Multiprotocol Wireless Sensor Networks, *Libelium, Spain.* www.libelium.com/?s=Long+Range+Multiprotocol+Wireless+Sensor+Networks

Salem Hadim and Nader Mohamed, (2006) Middleware for Wireless Sensor Networks: A Survey, IEEE First International Conference Communication System Software and Middleware, (*COMSWARE)*, New Delhi, India, pp.1-7.

José-Fernán Martínez, Jesús Rodríguez-Molina, Pedro Castillejo and Rubén de Diego, (2013), Middleware Architectures for the Smart Grid: Survey and Challenges in the Foreseeable Future, *Energies*, Vol. 6, No. 7, pp. 3593-3621.

D. Estrin, R. Govindan, J. S. Heidemann, and S.Kumar, (1999), Next century challenges: Scalable coordination in sensor networks, *in Proc. 5th Ann. Intl. Conf. on Mobile Computing and Networking. ACM/IEEE*, NewYork, USA, pp. 263-270.

J. Heideman, F, Silva, C. Intanagonwiwat, R.Govindan, D. Estrin, and D. Ganesan, (2001), Building Efficient Wireless Sensor Networks With Low-Level Naming. *ACM SIGOPS Operating Systems Review*, Vol. 35, No. 5, pp.146-159.

P. Levis and D. Culler, (2002), Mate: A Tiny Virtual Machine for Sensor Networks, *In ACM Sigplan Notices*, Vol. 37, No. 10, pp.85-95.

R. Barr, J.C. Bicket, D.S Dantas, B.Du, T.W.D. Kim, B. Zhou and E.G. Sirer, (2002), On the Need for System-Level Support for ad hoc and Sensor Networks, *ACM SIGOPS Operating Systems Review*, Vol. 36, No. 2, pp.1-5.

W.B. Heinzelman, A.L Murphy, H.S Carvalho and M.A Perillo, (2004), Middleware to Support Sensor Network Applications. *IEEE Network Magazine Special Issue*, Vol. 18, No. 1, pp.6-14.

Yong Yao, (2006), Cougar Project, *Cornell University*, NewYork, USA, www.cs.cornell.edu/database/cougar

C. Srisathapornphat, C. Jaikaeo and C. Shen, (2000), Sensor Information Networking Architecture. *IEEE International Workshops on Parallel Processing*, pp. 23- 30.

X. Yu, K. Niyogi, S. Mehrotra and N. Venkatasubramanian, (2003), Adaptive Middleware for Distributed Sensor Environments. *IEEE Distributed Systems*, Vol. 4, No. 5, pp.1541-4922.

Steven T. Karris, (2006), Introduction to Simulink® with Engineering Applications, *Orchard Publications*, pp. 16-56.